Structural phase transitions in bulk $YBa_2Cu_3O_{6+x}$ with $x=0.35$ and $x=0.36$

H. F. Poulsen,* M. von Zimmermann, and J. R. Schneider
Hamburger Synchrotronstrahlungslabor, HASYLAB at DESY, Notkestrasse 85, D-22603 Hamburg, Germany

N. H. Andersen, P. Schleger,† J. Madsen, R. Hadfield,‡ and H. Casalta§
Department of Solid State Physics, Risø National Laboratory, 4000 Roskilde, Denmark

Ruixing Liang, P. Dosanjh, and W. Hardy
Department of Physics, The University of British Columbia, Vancouver, British Columbia, Canada, V6T 1Z1
(Received 19 December 1995)

The structural behavior of mm^3-sized single crystals of $YBa_2Cu_3O_{6+x}$ with oxygen concentrations close to the metal-insulator transition is studied as a function of temperature, using 95-keV synchrotron x-ray diffraction. At $x=0.36$, no evidence is found of a room-temperature phase separation into tetragonal and orthorhombic phases, nor of a phase boundary between Ortho-II and tetragonal. Instead, we observe two distinct phase transitions: tetragonal to Ortho-I with a critical temperature $T_{OI}=246(2)$ °C and Ortho-I to Ortho-II with $T_{OII}=85(10)$ °C. Measurements of the spontaneous strain show the O/T transition to be nearly continuous with a critical exponent $\beta=0.34(2)$, consistent with a 3D Ising model driven weakly first order, presumably by the strain. A memory effect is observed, where relics of the twin domains—possibly related to tweed formations—continue to exist in the tetragonal phase when the temperature is increased above T_{OI}. Corresponding measurements for $x=0.35$ gave similar results—with $T_{OI}=181(2)$ °C, $T_{OII}=95(10)$ °C, and $\beta=0.35(2)$—but with the appearance of a small tetragonal component at room temperature. This component is interpreted as a nonequilibrium feature. In both cases the Ortho-I to Ortho-II transformations are very broad with a characteristic temperature dependence of the widths of the superstructure peaks that are similar to results obtained in a previous study for $x=0.50$. By comparison of the Ortho-II correlation lengths along a, b, and c with the corresponding data for $x=0.50$ we find evidence for a strong x dependency of *ASYNNNI*-type effective interaction parameters. The present results cannot be explained in terms of prevalent lattice gas models of the oxygen ordering and emphasizes the need for a theoretical basis that incorporates the strain and charge degrees of freedom. [S0163-1829(96)08421-4]

I. INTRODUCTION

The oxygen ordering in $YBa_2Cu_3O_{6+x}$ (YBCO),[1–33] as well as its connection to the superconducting properties,[34–37] has been the subject of a large number of studies. Nevertheless, questions concerning the relevant low-temperature part of the structural phase diagram, including the number of phases and the nature and position of the various phase lines, are still largely unsettled, mainly due to a series of experimental complications. These include the slow oxygen kinetics, the possible existence of metastable states, the impurity levels present (which recently has been suggested to be responsible for the lack of long-range order of the low-temperature Ortho-II phase[1]), and the difference in the minimal size of coherence volume that can be detected by various probes. As a result it has not been possible to perform thorough tests on the proposed models[2–4] of the oxygen ordering.

Among the unsettled issues are the exact nature of the orthorhombic-tetragonal (O/T) phase transition, and the related dynamic features. Hence, although the main driving force is clearly entropic, with the disordered oxygen atoms on the O(5) and O(1) sites becoming aligned in chains on the O(1) site in the orthorhombic phase,[5] the transition also has a paraelastic-ferrorelastic component, leading to twinning along ⟨110⟩ as well as tweed formations. As a result, one may define two order parameters: the site-order parameter, $\sigma=\{n[\mathrm{O}(1)]-n[\mathrm{O}(5)]\}/\{n[\mathrm{O}(1)]+n[\mathrm{O}(5)]\}$, and the spontaneous strain, $e=(b-a)/(a+b)$. It should be noted that the underlying mechanisms of vacancy hopping and phonon relaxation are associated with very different time and length scales.

Another open question is the exact structure (chain and cluster distributions) of the Ortho-II phase. Ultimately, this information is required in order to settle the ongoing dispute on the correlation between structure and superconductivity in this compound, including the question of the origin of the ''60 K plateau.'' The phase, which involves a doubling of the unit cell along the a axis, is stoichiometric only at $x=0.5$. It has never been observed to form a true long-range structure. Mapping out the phase lines and elucidating the mechanisms behind the ''phase transitions'' would be helpful in understanding the underlying thermomechanics. Some progress may here have been gained with our previous report on the temperature dependence of the diffuse Ortho-II superstructure peaks at $x=0.50$,[1] leading to the hypothesis of a random-field transition between Ortho-I and Ortho-II. However, this concept still awaits confirmation by additional experimental work. In any case, comparable data for a nonstoichiometric compound would be of interest.

In this work, we focus on the metallic part of the low-temperature phase diagram close to the metal-insulator transition. The popular *ASYNNNI* lattice-gas model,[3] which has

successfully explained the majority of the high-temperature features,[6,7] here predicts a single phase transformation directly from Ortho-II to tetragonal.[8] Initial work on this model based on cluster variation methods showed a miscibility gap between the two phases,[9–11] but later studies based on the more accurate transfer matrix or Monte Carlo simulation methods determined the transition to be of second order.[12,13] The lattice-gas model with screened Coulomb repulsions, suggested by Aligia *et al.*[4] gives rise to similar results.[14] In contrast to this, the model of Khachaturyan and Morris,[2] which assumes the Ortho-II phase to be transient, predicts a low-temperature spinodal decomposition into a tetragonal and an orthorhombic phase.

Here, we report on the first bulk single-crystal measurements of the structural behavior in this part of the phase diagram. We have chosen to use high-energy x-ray diffraction, since this technique combines a large penetration power and high flux with a high reciprocal space resolution. Hence, it allows us to monitor *in situ*, and on the same crystal, the statics and dynamics of two order parameters: e and $S_{O\mathrm{II}}$, where $S_{O\mathrm{II}}$ is the structure factor of one of the Ortho-II superstructure peaks. Moreover, a third-order parameter, σ, could in principle be measured on the same crystal using neutron diffraction, provided a monodomain crystal had been available. The use of large crystals allows for true bulk investigations and also makes it easier to minimize oxygen gradients developing during experiments, since in our case effectively no oxygen out-diffusion takes place in vacuum at the temperatures investigated. A further advantage is that a nondestructive technique, neutron four-circle refinements, can be used to determine the oxygen stoichiometry.

Due to the slow oxygen kinetics at low temperatures there exists a lower limit on x, below which it becomes impossible to study the O/T transition under equilibrium conditions. We estimated this limit to be at $x=0.35$, and prepared two crystals for the experiment with oxygen concentrations of 6.35 and 6.36.

II. SAMPLE PREPARATION AND CHARACTERIZATION

The two high-purity single crystals were grown in $SrTiO_3$ crucibles by a flux method using 99.999% pure chemicals. They are known to exhibit exceptionally good physical properties.[18] The crystals were reduced from the fully oxidigenated state in a gas-volumetric equipment[6] by use of a cryogenically assisted volumetric titration technique.[19] High-purity powder material is used as a buffer in the titration process. Water absorbed on the powder surface is removed by a liquid nitrogen wand at low oxygen pressure where oxygen condensation is precluded. During the titration process the oxygen stoichiometry is controlled and monitored by the oxygen pressure in the fixed system volume, and it is assured that the oxygen equilibrium pressure corresponds to the high-precision values given in Ref. 19. Adjustment of the oxygen stoichiometry is made at 600 °C where the oxidation kinetics is fast.[7] With the low oxygen equilibrium pressure at this point in the phase diagram, ($\approx$2 Torr), and the amount of powder and the system volume used in the preparation, essentially no changes in the oxygen stoichiometry will result during cooling. However, to allow for the oxygen ordering to take place, the YBCO materials are subsequently slowly cooled to room temperature. For the $x=0.36$ preparation the cooling rate was 20 °C/h, for $x=0.35$ it was 5 °C/h.

The crystal with $x=0.36$ had a weight of 60 mg with approximate dimensions $3.8\times3.0\times0.8$ mm^3, the $x=0.35$ crystal weighed 45 mg and had dimensions $2.9\times3.5\times0.7$ mm^3. The crystals were characterized at room temperature by standard single-crystal diffraction using the TAS 2 four-circle diffractometer at the DR3 reactor at Risø National Laboratory. A neutron wavelength of $\lambda=1.047$ Å was used and about 375 independent reflections were recorded and used to determine the crystallographic parameters, including the oxygen stoichiometry. For both crystals the oxygen stoichiometries determined from the gas-volumetric preparation and the diffraction data were in full agreement within the experimental error of $\Delta x=0.005$. Since the neutron diffractometer cannot resolve the twin peaks, only the average values of the a and b axes were determined. For the $x=0.36$ crystal we found $(a+b)/2=3.860$ Å and $c=11.776$ Å, and for $x=0.35$ $(a+b)/2=3.855$ Å and $c=11.781$ Å. The complete set of crystallographic data for the $x=0.36$ crystal is reported in Ref. 20. Similar results were found for the $x=0.35$ crystal. Values for a-b and for crystal mosaicities were determined using the high-energy x rays. For the $x=0.36$ crystal the HWHM in the $(a$-$b)$ plane is 0.065°. For the $x=0.35$ crystal the values are 0.095° in the $(a$-$b)$ plane, 0.055° in the $(a$-$c)$ plane, and 0.12° in the $(b$-$c)$ plane.

ac-susceptibility measurements were used to characterize the superconducting properties. Broad superconducting transitions were observed, in particular for the $x=0.35$ crystal where a small initial decrease is observed in the susceptibility at 60 K with a more rapid decline below 35 K. The susceptibility was not fully saturated at 15 K for this crystal. For the $x=0.36$ crystal the initial decline was at 39 K followed by a rapid decrease at 25 K with full saturation at 20 K. These very broad transitions are in contrast to the results obtained for other oxygen stoichiometries using the same type of crystals where transition widths less than 5 K was observed, and for fully oxidized crystals it is about 1 K.

III. INSTRUMENT

The experiments were performed at the high-energy triple-axis diffractometer at beam-line BW5 at HASYLAB.[38] The diffractometer has a (horizontal) dispersive Laue scattering geometry and is equipped with a standard Huber 512 Eulerean cradle and a solid-state Ge detector. At the time, the beamline was equipped with a symmetric Wiggler with a critical energy of 15.8 keV. No focusing elements were present. The energy spectrum below 40 keV was cut off by insertion of a 1.5-mm Cu plate in the beam in front of the monochromator. The measurements on the two crystals were done within a 6-month time interval, but under nearly identical circumstances. Here, we will summarize only the settings for the $x=0.36$ case.

The x-ray energy was 95 keV, corresponding to an attenuation length in the material of $\mu_{\mathrm{tot}}=0.85$ mm^{-1}. The illuminated part of the sample was determined by a tungsten diaphragm to be 2×2 mm. Two other diaphragms were inserted between sample and detector in order to reduce the background. The contamination of the signal from higher harmonics (on the order of 10^{-3}) was removed by the use of electronic windows.

Two setups were used throughout: a high-resolution one for characterizing the O/T transition, and a high-flux one for measurements related to the Ortho-II superstructure peaks. The high-resolution setup involved the use of two perfect Si (2,2,0) crystals as monochromator and analyzer crystals. The corresponding resolution for the YBCO (2,0,0) reflection was calculated to be 2×10^{-5} Å^{-1} (transverse) and 2×10^{-4} Å^{-1} (longitudinal) and 0.05 Å^{-1} (vertical). For the high-flux setting two imperfect $SrTiO_3$ crystals with HWHM's of approximately 15 arc sec [reflection: (2,0,0)] were used. The in-plane resolution for YBCO (2,0,0) was measured to be 2.3×10^{-4} Å^{-1} (transverse) and 6.1×10^{-3} Å^{-1} (longitudinal). The vertical resolution was in this case determined by the opening of the last diaphragm before the detector. In order to collect as much of the superstructure peak as possible, the opening was set to match nearly half a reciprocal-lattice unit along the c axis, that is 0.24 Å^{-1}. A detailed account of the relevant resolution calculations for the instrument is given in Ref. 21. Absolute values for $(a+b)/2$ and c were taken from the neutron four-circle work, while the synchrotron provided high accuracy values for the orthorhombicity.

For studies of the temperature dependence the sample was inserted in a small furnace and subject to an inert atmosphere of 0.3-bar Ar gas. The furnace was stable within 1°. With this equipment several heating and cooling cycles as well as quench experiments were performed, all within the temperature interval from 25 to 300 °C. Reproducibility of the data from repeated measurements shows that no change in the oxygen stoichiometry results from the thermal cycling.

IV. RESULTS

A. The Ortho-II superstructure

The diffuse scattering within a unit cell in reciprocal space was characterized at room temperature. For both crystals, the only features found were rather broad superstructure peaks related to the Ortho-II phase. A typical k scan through the (2.5,0, 0) reflection is shown in Fig. 1 for $x=0.36$. Also shown is the effective resolution, including the mosaicity of the sample, as determined from a k scan through (2,0,0). Along l the superstructure peaks were strongly overlapping. By fitting simple Lorentzians to the peak profiles, having corrected for the effective resolution, we find HWHM peak widths of $\Delta h=0.052(4)$, $\Delta k=0.0063(8)$, and $\Delta l=0.42(10)$ reciprocal-lattice units (r.l.u). Consistent with the Lorentzian line shape the corresponding correlation lengths defined by $1/\xi=\Delta Q_{\mathrm{HWHM}}$ are $\xi_a=12$ Å, $\xi_b=98$ Å, and $\xi_c=4.5$ Å. The scans for $x=0.35$ looked similar with resulting values of $\Delta h=0.050(4)$, and $\Delta l=0.25(8)$ and thereby $\xi_a=12$ Å and $\xi_c=7$ Å (Δk not measured).

The temperature dependence of the (2.5,0,0) peak intensity upon slow heating (25 °C/h) is shown in Fig. 2 for $x=0.36$. The peak intensity is seen to be constant up to 50 °C, and then to decrease slowly. At 200 °C the peak has still not completely vanished, but it becomes too broad to follow further up in temperature. The peak width along h, shown as an inset, remains constant until 85(10) °C, after which it broadens rapidly. Due to overlap and/or twinning the temperature dependence of the width in the two other directions could not be determined with sufficient accuracy. Upon slow cooling the original room-temperature values were regained.

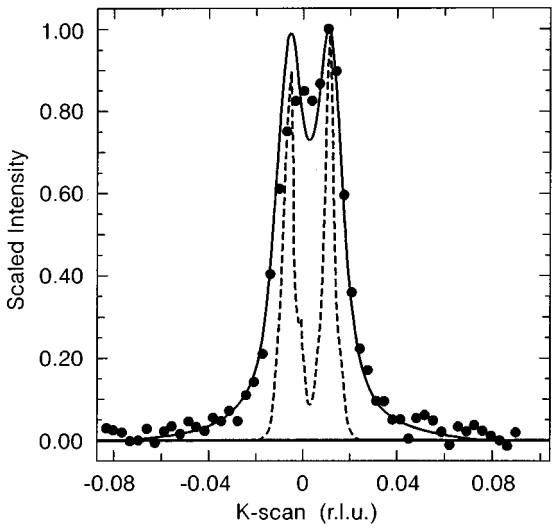

FIG. 1. A transverse (k) scan through the Ortho-II superstructure (2.5, 0, 0) of $YBa_2Cu_3O_{6.36}$. The scan, marked with dots, was performed at room temperature and with the a-b plane as the scattering plane. The dashed line represents the effective resolution as determined from a similar scan through the fundamental (2,0,0) reflection. The full line is a fit to two simple Lorentzians convoluted with the effective resolution. The split peaks are due to the twinning of the crystal. All scans have been normalized to 1 after subtraction of the background.

The corresponding results for $x=0.35$ are shown in Fig. 3. In this case the heating process was somewhat slower (10 °C/h), and the (2.5,0,5) peak was monitored instead of (2.5,0,0) where a spurious peak caused by multiple scattering was observed. Again, the peak intensity is seen to be con-

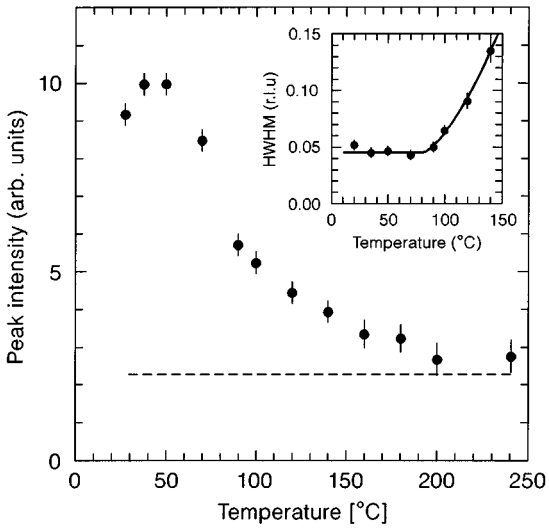

FIG. 2. The peak intensity of the $x=0.36$ (2.5, 0, 0) superstructure reflection as function of temperature on slow heating. The a-c plane is identical to the scattering plane. The dashed line marks the background. The corresponding evolution of the peak width (HWHM), measured along h, is shown as an inset. The full line in the inset is a guide to the eye.

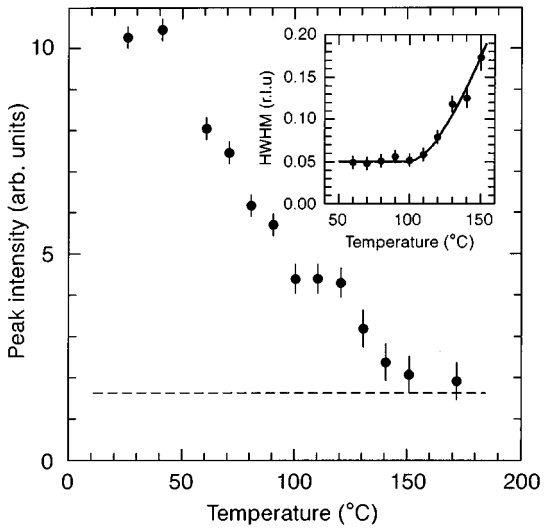

FIG. 3. The peak intensity of the $x=0.35$ (2.5, 0, 5) superstructure reflection as function of temperature on slow heating. The a-c plane is the scattering plane. The dashed line marks the background. The corresponding evolution of the peak width (HWHM), measured along h, is shown as an inset. The full line in the inset is a guide to the eye.

stant up to 50 °C, and then to decrease slowly. At 150 °C it has still not reached the background level. The peak width along h, shown as an inset, remains constant until 95(10) °C, after which it broadens rapidly. However, the peak width along l was found to start broadening around 80 °C.

B. The O/T transition, $x=0.36$

The intensity distribution in the $(a$-$b)$ plane around the fourfold-degenerate (2,0,0) reflection, that results from twinning, was characterized at room temperature. Some minute diffuse streaks were found along $\langle 1,0,0\rangle$ and $\langle 1,1,0\rangle$, which could be attributed to well-known resolution effects[21] and to scattering from the interfaces between the twin domains,[22,23] respectively. Apart from that, the crystal was single phase, in particular there was no evidence for any tetragonal component.

Next, measurements were performed of the diffuse scattering around (2,0,0) during heating and subsequent cooling through the O/T transition. Experimental time constraints did not allow us to perform full contour plots in the $(a$-$b)$ plane for each temperature. Instead we made longitudinal scans in the $(a$-$c)$ plane. Due to the poor vertical resolution this implied effectively an integration over the intensity distribution along k. The resolution along l, effectively the same as the ω resolution, was very fine. As the crystal orientation might change slightly in ω with temperature, the centering of the peaks was tested at selected temperatures.

The temperature was varied in the interval between 150 °C and 280 °C in steps of 3–10 °C with a speed of approximately 10 °C/h. Selected scans performed on heating are shown in Fig. 4. Between 25 °C and 235 °C the intensity distribution of the scans can all to a good approximation be fitted to a combination of two Bragg components and a central nearly flat intensity distribution, arising from the domain-wall scattering.[23] The intensity of the three components stays approximately constant with temperature, at least up to 210 °C, consistent with the behavior of single-phase orthorhombic material. Above 235 °C the intensity of the center part rises rapidly, and a third peak near the center evolves. The two ''orthorhombic'' peaks diminish and end up as shoulders on the central one, cf. the $T=260$ °C curve. Above 265 °C a single peak remains, consistent with single-phase tetragonal material.

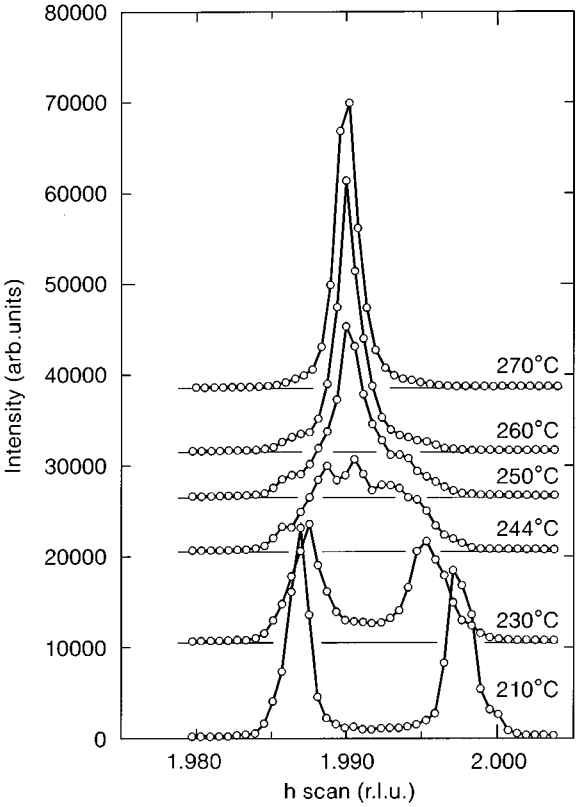

FIG. 4. Selected h scans through the degenerate (2,0,0)/(0,2,0) reflection on heating for $x=0.36$. The graphs have been displaced vertically and horizontally in order to ease the presentation. The solid lines marks the amount of vertical translation.

The mentioned peaks have been fitted to simple Lorentzians. The resulting variation of a and b with temperature is shown in Fig. 5, c was not measured. The position of the peaks were shown to be robust towards changes in the choice of fit function. A small but significant jump of $\Delta=8\times10^{-4}$ Å in the average lattice constant is evident at the phase transition. Shown in Fig. 6 are the corresponding data for the width of the peaks. The room-temperature HWHM values were 0.000 80 and 0.000 70 r.l.u. From the variation with temperature of the fitted HWHM's below 235 °C, we estimate that gradients of any sorts (temperature variations, oxygen inhomogenieties) at most can have 'broadened' T_{OI} by 5 °C. It follows that the mixed phase region, which is 30 °C broad, cannot be explained solely in terms of gradients.

The behavior shown in Fig. 4 was reproduced during subsequent cooling. With due respect to the statistical uncertainties the corresponding curves for the lattice parameter variation with temperature also look identical. In particular, there is no evidence for hysteresis in the lattice parameters. The difference in the orthorhombicity between before and after

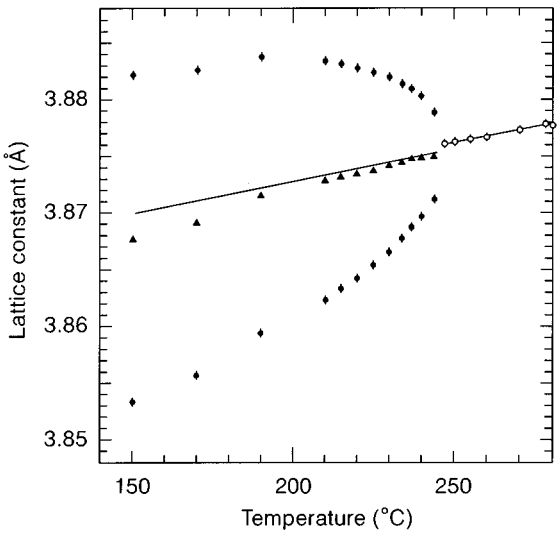

FIG. 5. Lattice constants, a and b, as function of temperature on heating for $x=0.36$. Full circles refer to the orthorhombic phase, open circles to the tetragonal phase. The average lattice constant in the orthorhombic phase is marked by triangles. Lines are linear fits to the points closest to the phase transition.

the heating cycle was less than 3×10^{-5}. It follows that oxygen out-diffusion is negligible in the temperature range used here.

The fitted values of the peak widths on cooling have been included in Fig. 6. In this case there is some evidence for hysteresis. It is also noteworthy that the width of the (2,0,0) tetragonal reflection at 280 °C is identical to the width of the orthorhombic (2,0,0) reflection at room temperature. [The width of (0,0,6) at 280 °C was, in the same units of $a^\star$, measured to be 0.000 50.] We interpret this as a memory effect, where relics of the twin domains continues to exist within the tetragonal phase within time intervals of at least days.

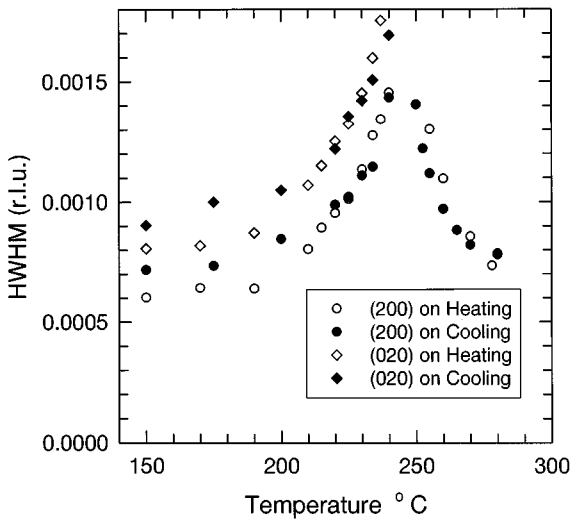

FIG. 6. Peak widths of longitudinal scans through the (2,0,0) and (0,2,0) reflections as function of temperature for $x=0.36$. Open and full symbols refer to heating and cooling conditions, respectively. The same symbol has been used for orthorhombic (200) and tetragonal (200)/(020). The instrumental resolution is of the order 0.0002 r.l.u.

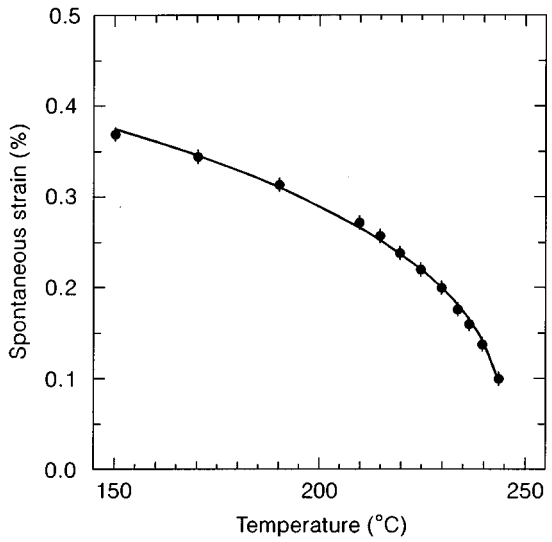

FIG. 7. Spontaneous strain, $e=(a-b)/(a+b)$, as function of temperature on heating for $x=0.36$. The line represents a fit to a simple scaling ansatz, as described in text.

The variation of the spontaneous strain with temperature on heating is shown in Fig. 7. Also shown is the result of a fit to a simple scaling law $e=\alpha[(T-T_{OI})/T_{OI}]^{\beta}$. A best fit was obtained for $T_{OI}=246(2)$ °C and $\beta=0.36(2)$. Corresponding values for cooling were $T_{OI}=247(2)$ °C and $\beta=0.33(2)$. Due to the small first-order component applying a simple scaling law is not strictly correct. Following Schlenker *et al.*,[29] fits should instead be done to $e_{11}=e+\Delta/(2a)=\alpha[(T-T_{OI})/T_{OI}]^{\beta}$. However with $\Delta/(2a)\approx10^{-4}$, no significant change is found in the fits.

Next, we investigated the dynamics. A set of quench experiments from 270 °C to various temperatures below 200 °C were performed. At each temperature we monitored the time evolution of h scans, similar to those in Fig. 4, during approximately an hour. However, for all temperatures the single-phase orthorhombic structure developed faster than the relaxation time of the furnace (approximately 2 min) allowed us to monitor. Consequently, there were no signs of any time evolution. In contrast, a time constant of the order of 1 h was observed at 247 °C, close to T_{OI}.

Finally, as a test of reproducibility the whole heating-cooling cycle was repeated twice. The second time 1 month later with a different furnace, an illuminated area of 0.2×0.2 mm^2 and a complete realignment of the diffractometer and the sample. The heating and cooling rates varied substantially between these cycles. In all cases, identical results were obtained (e.g., $T_{OI}=245$ °C and $T_{OI}=247$ °C on heating).

C. The O/T transition, $x=0.35$

The experiments performed on the $x=0.35$ crystal were quite similar to those performed on $x=0.36$. Again we characterized the diffuse scattering around the four Bragg peaks of one of the degenerate (2,0,0)/(0,2,0) reflections at room temperature. This was done after cooling slowly over a period of 12 h from 250 °C to 25 °C. The resulting intensity distribution in the $(a\text{-}b)$ plane is shown in Fig. 8. The diag-

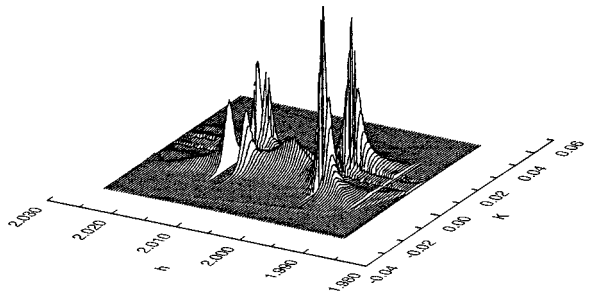

FIG. 8. Intensity distribution around the four times degenerate (2,0,0) reflection for $x=0.35$. The figure is based on 23 k scans in the $(a\text{-}b)$ plane at room temperature. The areas around the center of the four Bragg peaks are left out. Between the Bragg peaks two diagonal streaks are evident, with a minor peak at the center. This diffuse scattering is interpreted as being the superposition of a small tetragonal composant and streaks related to scattering from the interfaces between twin domains.

onal streaks along [1,1,0] and [1,−1,0], which are always found in twinned crystals,[22,23] are supplemented by a small peak at the center. The streaks are caused by scattering from twin domain walls. Using the model of Salje and co-workers[22] with tanh-type strain fields around the domain walls, we find that the peak at the center cannot be explained in terms of the twin domains. Instead, we interpret it in terms of a tetragonal component, and estimate the integrated intensity of this component to be 4% of integrated intensity of the 4 orthorhombic Bragg peaks. (Alternatively, a more complex domain structure might be the origin of the peak.) A more detailed account of our analysis of the diffuse scattering will be given elsewhere.[23]

The temperature variation was done in 14 nonequidistant steps between 25 °C and 250 °C. In addition to h scans through (2,0,0) in the $(a\text{-}c)$ plane, the c axis was also monitored by l scans through the (0,0,6) reflection. The total duration of each temperature step was 35 min. Selected scans performed on heating are shown in Fig. 9. Again a transition zone of 20°–30° is found. However, compared with the $x=0.36$ case, all features are more smeared out in this case, i.e., we find no equivalent of the plateaus on the shoulder of the tetragonal peak as shown in Fig. 4 for $T=260$ °C. Actually, in this case we cannot exclude that the two-phase behavior is caused by inhomogeneities.

The difference between the two samples are seen more clearly in Fig. 10 where we compare h scans through (2,0,0) for $x=0.35$ and 0.36. Temperatures have been chosen such that the orthorhombicity is nearly the same for the two scans. From the figure it is evident that the orthorhombic peaks are broader near the base of the peaks for $x=0.35$, and that the scattering between the peaks are higher also for $x=0.35$. On top of this comes the small tetragonal component, which we know to be positioned near the center of the $x=0.35$ scan, cf. Fig. 8. These conclusions are independent of the criteria used for choosing which temperatures to compare (e.g., the features look the same when comparing scans at equal temperature difference from T_{OI}).

The measured peaks were again fitted to simple Lorentzians. The resulting variation of a, b, and c with temperature is shown in Fig. 11. c varies continuously through the transition, but with a distinct jump of $\Delta\alpha=3\times10^{-6}$ K^{-1} in the linear expansion coefficient at T_{OI}. Another small jump of -5×10^{-4} Å is evident in $(a+b)/2$ at the phase transition. The corresponding curve for cooling looks similar, e.g., with a jump of -7×10^{-4} Å in $(a+b)/2$. Again there is no evidence for hysteresis within the accuracy of the measurement.

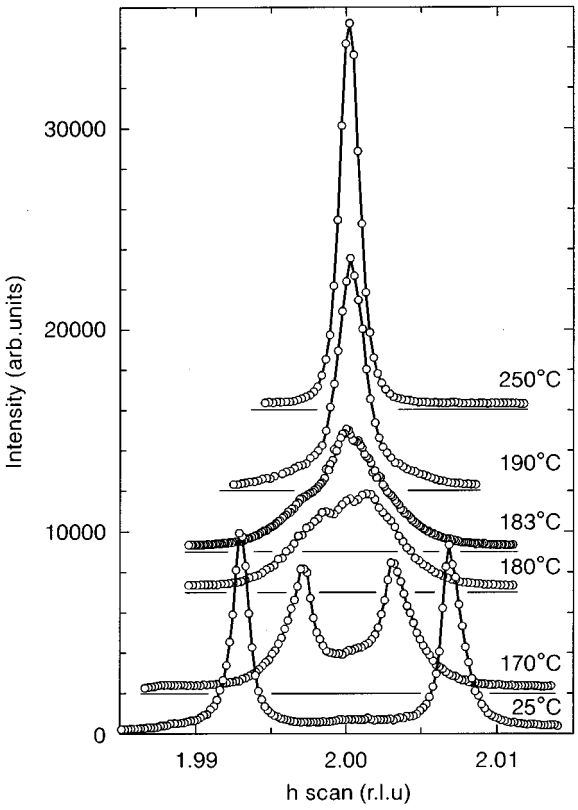

FIG. 9. Selected h scans through the degenerate (2,0,0)/(0,2,0) reflection on heating for $x=0.35$. The graphs have been displaced vertically and horizontally in order to ease the presentation. The solid lines marks the amount of vertical translation.

The measured widths (HWHM) of the (2,0,0), (0,2,0), and (0,0,6) reflections are shown as function of temperature in Fig. 12. In a small temperature interval around T_{OI}, where the overlapping between peaks is too severe, data have been left out. We note that the width of the c axis is temperature independent, and that the (2,0,0) and (0,2,0) peaks initially become narrower during heating. The latter effect is interpreted as a consequence of the crystal being in a nonequilibrium state at room temperature. As for $x=0.36$ there is evidence for hysteresis, but more pronounced in this case. The tetragonal width at the maximum temperature is again seen not to decrease below the ''orthorhombic level.'' The final peak widths of the two orthorhombic (2,0,0)/(0,2,0) components at 25 °C is 0.000 64 and 0.000 77 r.l.u., while the width of the tetragonal component at 250 °C is 0.000 74 r.l.u. These values are nearly identical to the $x=0.36$ ones.

The resulting spontaneous strain as function of temperature on heating is shown in Fig. 13. Also shown is a fit to $e=\alpha[(T-T_{OI})/T_{OI}]^{\beta}$. Best fits were obtained for $T_{OI}=183(2)$ °C and $\beta=0.35(2)$. The corresponding values for cooling were $T_{OI}=179(2)$ °C and $\beta=0.36(2)$. The difference in the room-temperature orthorhombicity between before and after the heating was within 10^{-4}.

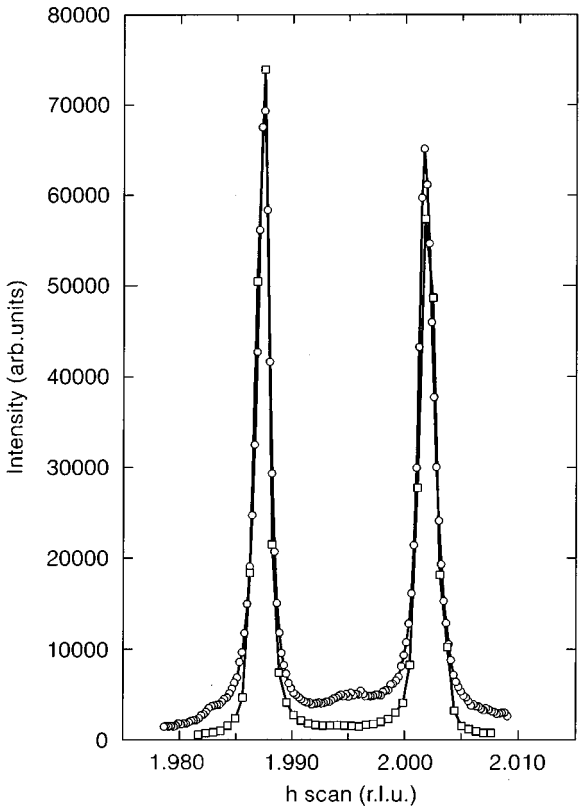

FIG. 10. Comparison of h scans through (2,0,0) in the (a-c) plane for $x=0.36$ (□) and $x=0.35$ (○). The scans were made during heating at constant temperatures of $T=150$ °C and $T=25$ °C for 0.36 and 0.35, respectively. The temperatures were chosen such that the orthorhombicity was nearly the same. The x axis refers to the $x=0.36$ sample. A small contraction of the $x=0.35$ graph axis has made it possible to align the peaks to each other. The scans are scaled, after background subtraction, such that the peak intensities are roughly equal.

V. DISCUSSION

The results for the O/T transition at $x=0.36$ represent close-to-equilibrium behavior. This follows from the facts that identical results were obtained for substantially different cooling rates and gauge volumes, that quench experiments revealed no transient behaviour, and that no hysteresis were observed in the lattice parameters. The structural data for $x=0.35$ on the other hand are believed to represent behavior somewhat further away from equilibrium. This is indicated by the initial drop in the (2,0,0) peak width on heating, by the larger amount of hysteresis in the widths of the peaks (cf. Figs. 6 and 12), and by the more pronounced broadening at the base of the orthorhombic peaks (cf. Fig. 10). The difference in behavior may readily be explained in terms of either the slower kinetics at T_{OI} for $x=0.35$ or in terms of larger structural fluctuations at $x=0.35$ caused by the proximity to the metal-insulator transition.

It follows that the observed features for $x=0.36$ are the more reliable ones. In particular, the small tetragonal component at $x=0.35$ might be a nonequilibrium feature. In fact, we believe this to be the case, as we lack a physical explanation of why a mixed-phase behavior only should be manifest at $x=0.35$. Clearly, in order to confirm this picture, it would be relevant to observe the time behavior of any even-

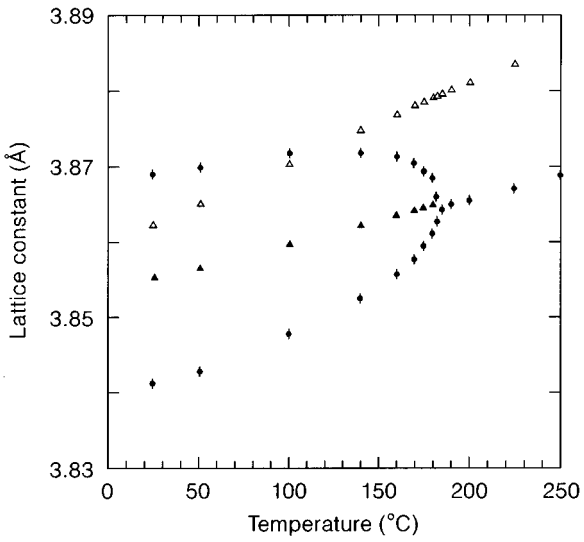

FIG. 11. Lattice constants, a, b, and $c/3.05$ as function of temperature on heating for $x=0.35$. Full circles refer to the orthorhombic phase, open circles to the tetragonal phase. The average lattice constant in the orthorhombic phase is marked by full triangles. Open triangles marks c divided by scale factor 3.05.

tual tetragonal components in future experiments. Alternatively, the peak might be caused by a more complex domain structure.

The study of Veal and co-workers[35] has some resemblance to the present one. They studied the structural evolution of small single YBCO crystals with $x=0.30$, 0.35, and 0.45 as function of aging in air at room temperature after quenches from 520 °C, that is from the tetragonal to Ortho-II

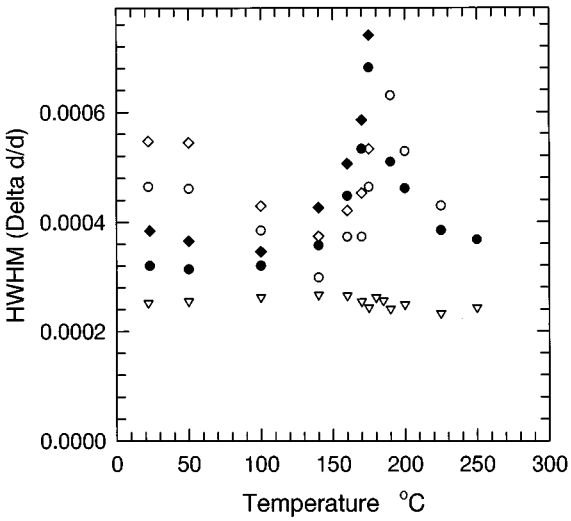

FIG. 12. Peak widths of longitudinal scans through the (2,0,0), (0,2,0), and (0,0,6) reflections a function of temperature for $x=0.35$. The widths ΔQ_{HWHM} have been normalized to the Bragg reflections as $(\Delta d)/d=(\Delta Q_{\mathrm{HWHM}})/Q$. Open and full circles refer to heating and cooling conditions, respectively. Circles mark (2,0,0), rhombs (0,2,0), and triangles (0,0,6) data. The same symbol is used for orthorhombic (2,0,0) and tetragonal (2,0,0)/(0,2,0). The data for (0,0,6) on cooling are within experimental error identical to the ones for heating shown here. The instrumental resolution is in all cases of the order $(\Delta d)/d=10^{-4}$.

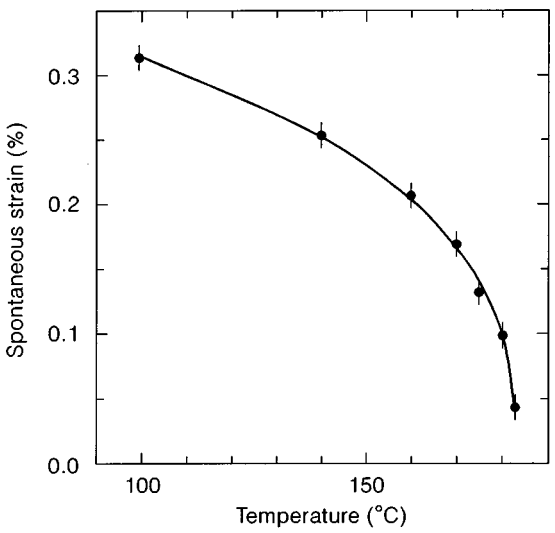

FIG. 13. Spontaneous strain as function of temperature on heating for $x=0.35$. The line represents a fit to a simple scaling ansatz, as described in text.

phase. Their results are consistent with a slow annealing out of ''tetragonal components'' and a corresponding sharpening of the orthorhombic peaks, the opposite behavior of what would result from phase separation. However, their final peak widths for $x=0.35$ are 2.3 times broader than the close-to-equilibrium data presented here.

It is also interesting to compare with two neutron powder diffraction studies. In the first one, YBCO powders were slowly cooled from 725 °C in a controlled atmosphere at nearly constant stoichiometry.[6] This was done on-line on the diffractometer. The resulting transition temperatures correspond to the present ones within experimental accuracy ($\Delta x=0.01$). Within the poor longitudinal resolution of this experiment the structures were single phase. In the second one, Radaelli *et al.*[16] slowly cooled $ErBa_2Cu_3O_{6+x}$ powders from 400 °C in order to make diffractograms at room temperature. The yttrium and erbium compounds are believed to be nearly identical as the ionic radius of Y and Er in eightfold coordination is 1.019 and 1.004 Å, respectively. They reported on two-phase behavior in the whole range $0.25<x<0.45$ with much larger volume fractions of tetragonal phase than found here and with a pronounced broadening of the c axis around the transition. We take the difference in results as evidence for the importance of using high-quality single crystals and careful annealing procedures in this part of the phase diagram. (Their starting material was a mixture of tetragonal and orthorhombic powders. Sintering at 400 °C may not have been sufficient to ensure a fully homogeneous powder.)

Our results are also very different from the outcome of the ultra-high-resolution electron microscopy study of Horiuchi,[17] who reported on large regions (20–100 Å) of pure tetragonal phase in the outer 15–30 Å layer in YBCO at $x=0.40$. Based on the present studies it is questionable whether their results are representative of bulk equilibrium behaviour. The extensive room-temperature TEM study by Beyers *et al.*,[26] on the other hand, did not show any multiphase behavior in this part of the phase diagram.

Turning to the nature of the O/T transition, we start by assuming it to be continuous. Then we note that the active irreducible representation of the $P4/mmm$-$Pmmm$ transition is B_{1g}. The symmetry of σ and e are identical, and a bilinear coupling is allowed at the Γ point. The measured values of the critical parameter β may therefore be compared directly with the theoretical three-dimensional (3D) Ising value of $\beta=0.326$, generally expected to be valid provided the transition is driven solely by the entropic forces. Within the listed uncertainties it is seen that the values correspond reasonably.

Next, we note that the 30° mixed-phase region around T_{OI} and the jump in the average lattice parameters for $x=0.36$, cf. Figs. 4 and 7, cannot be explained in terms of say a Gaussian or Lorentzian oxygen concentration distribution. The jump reproduced after diminishing the gauge volume to 1/100 of the original. These facts strongly suggest that the phase transition is weakly first order. However, a complete (dynamical) description of the interaction between the entropy and strain terms cannot be made before the time and temperature variations of both σ and e are measured on the same single crystal, e.g., by a combination of high-energy x-ray and neutron diffraction. Such studies are planned. Additional studies are also needed in order to elucidate to what extent the hysteresis of the peak widths and the mentioned memory effect is related to formation of tweed structures.

Experimentally, various neutron-diffraction work suggests that the O/T transition is second order in e throughout the phase diagram.[5,6,15,16] However, the Q-space resolution was in all cases too poor to resolve effects of the present type. On the other hand, several TEM studies indicate discontinuities. As an example Schmahl *et al.*[25] studied a series of Co-doped compounds $YBa_2(Cu_{1-y}Co_y)_3O_{6+x}$ at room temperature. At the O/T transition concentration of $y=0.025$ a small jump of $\Delta=0.0018$ Å was found in $(a+b)/2$. The doped compounds are known to be nearly fully oxygenated. Provided temperature and chemical concentration are equivalent driving forces, their data therefore imply that the O/T transition in pure YBCO near $x=1.0$ is first order.

In terms of σ, existing high-temperature neutron powder data are consistent with a continuous transition,[5] while the previously mentioned low-temperature study by Radaelli *et al.*[16] gave evidence for a dramatic jump of $\Delta\sigma=0.6$ at the room-temperature transition. These results may to some extent be biased by errors on the occupation numbers, and possibly nonequilibrium behavior. However, taking them at face value they suggest the existence of a turnover from first-order to second-order behavior on the O/T phase line. Provided such a transition point exists, it is likely to be situated close to $x=0.5$, as there exists a number of experimental reports on anisotropies in the low-temperature properties at this concentration. Hence, Poulsen *et al.* give evidence for a change in the relaxation time for oxygen in-diffusion in powders[7] at $x=0.5$. Claus *et al.*[27] report that the difference in superconducting transition temperature between crystals annealed at 25 °C, and crystals annealed at 230 °C and then quenched to room temperature, are much larger for $x<0.5$. Moreover, Beyers *et al.* reports on Ortho-II superstructure reflections in TEM images being much sharper for $x>0.5$ than below.[26]

Theoretically, the appearance of a first-order component is typical for systems with strain degrees of freedom.[39] Sev-

eral attempts has been done to incorporate these within a Landau formalism based on (simplified versions of) the *ASYNNNI* model.[25,28,30] However, a full treatment has to our knowledge not been performed, due to, e.g., missing information on the elastic coefficients and their temperature dependence within the various low-temperature phases. From the square-rectangular symmetry breaking itself, Blagoev and Wille[28] nevertheless inferred that the Ortho-I to Ortho-II transition becomes first order while the O/T transition remains continuous. Günther *et al.* actually managed to drive the O/T transition first order[30] but only by introducing *ad hoc attractive* interactions beyond the next-nearest-neighbor distance.

Turning next to the data on the superstructure peaks, we start by comparing with the results from one of our earlier experiments.[1] In that study the temperature dependence of the diffuse scattering was examined in great detail for an $x=0.50$ crystal from a batch prepared under identical circumstances. The results for the temperature dependency of the intensities and widths (cf. Figs. 2 and 3) are very similar. In particular, the existence of an ''onset'' temperature above which the peak widths starts to widen considerably. This ''onset'' temperature was defined as the transition temperature $T_{O\mathrm{II}}$, which in the case of $x=0.50$ was 125 °C. Another of the characteristics of the $x=0.50$ data was a shift in the peak shape from a Lorentzian type above $T_{O\mathrm{II}}$ to a Lorentzian square type well below. Such behavior is found on a qualitative basis to be consistent also with the present data. We therefore conclude that the Ortho-I to Ortho-II transition at $x=0.35$ and 0.36 might be governed by the same mechanisms as the transition at $x=0.50$, but with the lower transition temperatures of $T_{O\mathrm{II}}=95(10)$ °C and $T_{O\mathrm{II}}=85(10)$ °C, respectively. A correlation of these results to the hypothesis of a random field transition[1] will be done elsewhere.

It follows that it also is meaningful to compare the room-temperature Ortho-II peak widths with the previous study. At $x=0.50$ we had (HWHM) $\Delta h=0.0103$, $\Delta k=0.002\,74$, and $\Delta l=0.0674$ r.l.u. Hence, the correlations along h and l as compared with those along k are much weaker at the present stoichiometries. (On heating the $x=0.5$ sample the ratios ξ_a/ξ_b and ξ_c/ξ_b became larger. The difference between the samples therefore cannot be explained simply in terms of different ''effective quench temperatures.'') Within the framework of the *ASYNNNI* model, this fact suggests that the effective pair interactions varies with the oxygen concentration.[33]

Concerning the Ortho-I–Ortho-II transition, the work of Gerdanian and Picard[24] is to our knowledge the only previous experimental study related to this part of the phase diagram. They inferred the transition temperature from kinks in Seebeck measurements on powders. Adjusting for a small difference in the absolute x values, such that $T_{O\mathrm{I}}$ corresponds in the two studies, Gerdanian and Picard has $T_{O\mathrm{II}}=200$ °C for $x=0.36$. We attribute the 120 K difference in $T_{O\mathrm{II}}$ to difficulties in interpreting the Seebeck data.

The most notable of the present results are the single-phase orthorhombic structure at $x=0.36$, the weak first-order O/T transition, the large separation between $T_{O\mathrm{I}}$ and $T_{O\mathrm{II}}$, the characteristic broad Ortho-I to Ortho-II transition and the evidence for an x dependence of the ratio between the correlation lengths. In total, these findings are in contrast to predictions from prevalent models. They add to a series of studies that all emphasize that a satisfactory theoretical understanding of the oxygen ordering in YBCO still is lacking.[1,31,32] One of the problems is that lattice-gas models like the *ASYNNNI* model do not include charge and strain degrees of freedom. The former have been shown to be essential for understanding thermodynamic data[31] and the magnetic phase diagram.[32] The latter is stipulated here to be responsible for the crossover to first-order behavior of the O/T transition.

Finally, we note that the proof of the existence of an Ortho-I phase in between the tetragonal and the Ortho-II phases at $x=0.36$ opens up for renewed investigations along the lines of Veal *et al.*[35,27] In their often cited work they reported on the simultaneous evolution of structural parameters and superconducting transition temperature as function of time following a quench from slightly above $T_{O\mathrm{I}}$ to room temperature at various x values close to the metal-insulator transition. Two models were proposed for the relevant oxygen ordering and charge-transfer process, one based on the distribution of single-site Cu valences in the basal plane,[37] and one based on growth of Ortho-II domains.[36] A redesigned experiment, with the quench performed from a temperature between $T_{O\mathrm{I}}$ and $T_{O\mathrm{II}}$ down to room temperature, would allow one to distinguish between these models.

VI. CONCLUSIONS

The novel technique of high-energy synchrotron diffraction was used for the first detailed single-crystal *in situ* measurements of two of the three relevant order parameters: σ, e, and $S_{O\mathrm{II}}$. By preparation of monodomain crystals, all three parameters may be measured simultaneously in the future by combining the technique with neutron diffraction. The overall result of the present study is that of two distinct phase transitions: from tetragonal to Ortho-I and from Ortho-I to Ortho-II. The transition temperatures are $T_{O\mathrm{I}}=181$ °C and $T_{O\mathrm{II}}=95$ °C for $x=0.35$ and $T_{O\mathrm{I}}=246$ °C and $T_{O\mathrm{II}}=85$ °C for $x=0.36$. The measurements related to the O/T transition are consistent with a 3D Ising behavior driven weakly first order, presumably by the strain degrees of freedom. At room temperature the material is single-phase orthorhombic, at least at $x=0.36$. The Ortho-I to Ortho-II transition is very broad, with a characteristic variation of the peak widths versus temperature, previously found also at $x=0.50$. By further comparison to the $x=0.50$ data we find evidence for an x dependency in the ratio between Ortho-II correlation lengths. Finally, we note a marked memory effect, where relics of the twin domains continue to exist within the tetragonal phase above $T_{O\mathrm{I}}$.

ACKNOWLEDGMENTS

Fruitful discussions with Professor U. Bismayer, Professor W. W. Schmahl, and Dr. P. A. Lindgard are greatfully acknowledged. This work is supported by the EEC science and Esprit programs and the Danish Ministry of Energy.

*Present address: Materials Department, Risø National Laboratory, 4000 Roskilde, Denmark. Phone: +45-4677-5700; Electronic address: h.poulsen@risoe.dk

†Present address: Institute Laue-Langevin, B.P. 156, 38042 Grenoble Cedex, France.

‡Present address: Laboratoire de Cristallographie, CNRS, B.P. 166, 38042 Grenoble Cedex 09, France.

§Present address: Laboratoire Léon Brillouin, CE-Saclay, 91191 Gif-sur-Yvette, France.

[1] P. Schleger, R. Hadfield, H. Casalta, N. H. Andersen, H. F. Poulsen, M. von Zimmermann, J. R. Schneider, R. Liang, P. Dosanjh, and W. N. Hardy, Phys. Rev. Lett. **74**, 1446 (1995).

[2] A. G. Khachaturyan and J. W. Morris, Jr., Phys. Rev. Lett. **61**, 215 (1988).

[3] D. de Fontaine, L. T. Wille, and S. C. Moss, Phys. Rev. B **36**, 5709 (1987); D. de Fontaine, G. Ceder, and M. Asta, Nature **343**, 544 (1990).

[4] A. A. Aligia, A. G. Rojo, and B. R. Alascio, Phys. Rev. B **38**, 6604 (1988); A. A. Aligia and C. Ventura, Phys. Rev. Lett. **65**, 2475 (1990); A. A. Aligia, J. Garces, and H. Bonadeo, Phys. Rev. B **42**, 10 226 (1990).

[5] J. D. Jorgenson, M. A. Beno, D. G. Hinks, L. Soderholm, K. J. Volin, R. L. Hitterman, J. D. Grace, I. K. Schuller, C. E. Segre, K. Zhang, and M. S. Kleefisch, Phys. Rev. B **36**, 3608 (1987).

[6] N. H. Andersen, B. Lebech, and H. F. Poulsen, Physica C **172**, 31 (1991).

[7] H. F. Poulsen, N. H. Andersen, and B. Lebech, Physica C **173**, 397 (1991).

[8] For the *ASYNNNI* model, we assume the effective pair interactions have to obey the following inequalities: $V_2<0<V_3<V_1$. This relationship can be rationalized easily on chemical grounds, and is generally accepted.

[9] L. T. Wille, A. Berera, and D. de Fontaine, Phys. Rev. Lett. **60**, 1065 (1988).

[10] R. Kikuchi and J.-S. Choi, Physica C **160**, 347 (1989).

[11] V. E. Zubkus, S. Lapinskas, and E. E. Tornau, Physica C **159**, 501 (1989); V. E. Zubkus, E. E. Tornau, S. Lapinskas, and P. J. Kundrotas, Phys. Rev. B **43**, 13 112 (1991).

[12] T. Aukrust, M. A. Novotny, P. A. Rikvold, and D. P. Landau, Phys. Rev. B **41**, 8772 (1990).

[13] N. C. Bartelt, T. L. Einstein, and L. T. Wille, Phys. Rev. B **40**, 10 759 (1989).

[14] A. A. Aligia and J. Garces, Physica C **194**, 223 (1992). If λ depends on x, the phase diagram is modified as in V. E. Zubkus *et al.*, *ibid.* **198**, 141 (1992).

[15] J. D. Jorgenson, B. W. Veal, A. P. Paulikas, L. J. Nowicki, G. W. Crabtree, H. Claus, and W. K. Kwok, Phys. Rev. B **41**, 4 (1990); **41**, 1863 (1990).

[16] P. G. Radaelli, C. U. Segre, D. G. Hinks, and J. D. Jorgenson, Phys. Rev. B **45**, 3 (1992); **45**, 4923 (1992).

[17] S. Horiuchi, Jpn. J. Appl. Phys. **31**, L1335 (1992).

[18] R. Liang, P. Dosanjh, D. A. Bonn, D. J. Baar, J. F. Carolan, and W. N. Hardy, Physica C **195**, 51 (1992).

[19] R. Schleger, W. N. Hardy, and B. X. Yang, Physica C **176**, 261 (1991).

[20] H. Casalta, P. Schleger, P. Harris, B. Lebech, N. H. Andersen, R. Liang, P. Dosanjh, and W. N. Hardy, Physica C **258**, 321 (1996).

[21] H. F. Poulsen, U. Rütt, M. von Zimmermann, T. Kracht, and J. R. Schneider (unpublished).

[22] J. Crosh and E. K. H. Salje, Physica C **225**, 111 (1994).

[23] H. F. Poulsen, M. von Zimmermann, N. H. Andersen, and J. R. Schneider (unpublished).

[24] P. Gerdanian and C. Picard, Physica C **204**, 419 (1993).

[25] W. W. Schmahl, A. Putnis, E. Salje, P. Freeman, A. Graeme-Barber, R. Jones, K. K. Singh, J. Blunt, P. P. Edwards, J. Loram, and K. Mirza. Philos. Mag. Lett. **60**, 6 (1989); **60**, 241 (1989).

[26] R. Beyers, B. T. Ahn, G. Gorman, V. Y. Lee, S. S. P. Parkin, M. L. Ramirez, K. P. Roche, J. E. Vasquez, T. M. Gur, and R. A. Higgins, Nature **340**, 619 (1989).

[27] H. Claus, S. Yang, A. P. Paulikas, J. W. Downey, and B. W. Veal, Physica C **171**, 205 (1990).

[28] K. B. Blagoev and L. T. Wille, Phys. Rev. B **48**, 9 (1993); **48**, 6588 (1993).

[29] J. L. Schlenker, G. V. Gibbs, and M. B. Boisen, Acta Crystallogr. A **34**, 52 (1978).

[30] C. C. A. Günther, P. A. Rikvold, and M. A. Novotny, Phys. Rev. B **42**, 10 738 (1990).

[31] P. Schleger, W. N. Hardy, and H. Casalta, Phys. Rev. B **49**, 514 (1994).

[32] G. Uimin, Int. J. Mod. Phys. B **6**, 2291 (1992).

[33] T. Fiig, N. H. Andersen, P.-A. Lindgard, J. Berlin, and O. G. Mouritsen, Phys. Rev. B (to be published).

[34] R. J. Cava, A. W. Hewatt, E. A. Hewatt, B. Batlogg, M. Marezio, K. M. Rabe, J. J. Krajewski, W. F. Peck, Jr., and L. W. Rupp, Jr., Physica C **165**, 419 (1990).

[35] B. W. Veal, H. You, A. P. Paulikas, H. Shi, Y. Fang, and J. W. Downey, Phys. Rev. B **42**, 10 (1990); **42**, 6305 (1990); J. D. Jorgensen, S. Pei, P. Lightfoot, H. Shi, A. P. Paulikas, and B. W. Veal, Physica C **167**, 571 (1990).

[36] H. F. Poulsen, N. H. Andersen, J. V. Andersen, H. Bohr, and O. G. Mouritsen, Phys. Rev. Lett. **66**, 465 (1991); H. F. Poulsen, N. H. Andersen, J. V. Andersen, H. Bohr, and O. G. Mouritsen, Nature **349**, 594 (1991).

[37] B. W. Veal and A. P. Paulikas, Physica C **184**, 321 (1991).

[38] R. Bouchard, T. Schmidt, H. F. Poulsen, T. Kracht, H.-B. Neumann, U. Rütt, and J. R. Schneider (unpublished).

[39] A. D. Bruce and R. A. Cowley, *Structural Phase Transitions* (Benjamin, Menlo Park, 1984), pp. 23–26.